International Journal on Recent and Innovation Trends in Computing and Communication
ISSN: 2321-8169 Volume: 11 Issue: 9
Article Received: *25 July 2023* ***Revised:*** *12 September 2023* ***Accepted:*** *30 September 2023*

Detection of Diabetic Retinopathy Through Identification of Blood Vessel Thickness Using-FOFF

G.Indira Devi
Electronics and Communication Engineering
Anil Neerukonda Institute of Science and Technology
Visakhapatnam, India
e-mail: gedela.indira@gmail.com

D.Madhavi
Department of ECE, GIT
GITAM University
Visakhapatnam,India
e-mail: mdunna@gitam.edu

Abstract—Diabetes is one of the main problems in today's medical industry. Identification and diagnosis of the eye condition brought on by diabetes' elevated blood sugar levels are crucial. The motive of the work is to present a useful technique for system diagnosis utilizing a retinal fundus picture. A four-stage implementation paradigm is created in this study. Initially the input image is pre-processed, secondly blood vessel segmentation is performed; thirdly feature extraction and finally classification. In this paper an effective methodology is utilized by introducing meta heuristic algorithm. In the entire process, blood vessel segmentation (BVS)contributes a crucial part in DR detection for which a firefly optimized frangi filter (FOFF) is designed in this paper. The process of categorization comes last. The classifiers K-Nearest Neighbor (KNN) and Support Vector Machine (SVM) are employed. The performance of system is evaluated by computing the accuracy and precision. The results are compared between the two utilized classifiers. The SVM performance is good with an accuracy of 95.5% and KNN having an accuracy of 91.6%.

Keywords-Diabetic Retinopathy; Frangi Filter; Firefly optimization; KNN; SVM.

I. INTRODUCTION

Using blood vessel segmentation on fundus retinal pictures, clinicians may more accurately diagnose a variety of eye conditions. For an appropriate examination of the primary blood arteries and their branches, precise and complete blood vessel segmentation is required [1]. Currently, doctors designate blood arteries manually based on their experiences, which is inefficient and vulnerable to subjective influence [2]. The automated segmentation of retinal arteries is therefore very significant [3]. The segmentation of blood vessel is first introduced by author in [4] using Gaussian filter. The author of [5] then suggested a segmentation approach that incorporated a dual-threshold method with a multiscale matching filter. In [6], the author put forth a segmentation technique based on a grey co-occurrence matrix and a gabor filter. The multiscale 2D Gabor wavelet was used by the author in [7] to analyze the coarse and fine blood arteries. An approach based on the extended matched filter was suggested in [8]. In [9], the author used segmenting with a multiscale Gabor filter (GF) and thresholding approach based on multi-objective optimization to segment blood arteries.

By utilizing the GF and derivatives of the Gaussian distribution discussed by the author in [10] and improved the profile and structure of the blood vessels. The segmentation of retinal vessels needs to be improved for which the author of [11] presented a matched filtering strategy centered on the Gumbel PDF. These window-based techniques can preserve the original vessel structure, but because each pixel must be processed, there is a significant increase in computing effort and segmentation time. The Hessian matrix was utilized by the author in [12] to extract the distinctive directions of pictures. Based on the intrinsic properties of LoG and MF, the author of [13] retrieved blood vessels from retinal pictures, avoiding the incorrect categorization of nonvascular pixels. In [14], the author suggested a multiscale vascular segmentation approach based on continuity function of wavelet transform.

A level set and regional growth-based algorithm was proposed by the author in [15]. In [16], the author suggested a segmentation method for retinal arteries that included skeletonization, fuzzy entropy, and adaptive filtering. An approach to improve fine blood arteries through vascular area and axial ratio was put out in [17]. The information from the picture hybrid area was used by the author in [18] to construct an endless activity profile model for retinal vascular segmentation. These vessel tracking systems can collect specific blood vessel local characteristics. However, because of branching or intersections, they are unable to achieve

International Journal on Recent and Innovation Trends in Computing and Communication
ISSN: 2321-8169 Volume: 11 Issue: 9
Article Received: *25 July 2023* ***Revised:*** *12 September 2023* ***Accepted:*** *30 September 2023*

continuous tracking, which leads to inaccurate segmentation. In [19], the author put out a wavelet transform and mathematical morphology-based approach for optic disc identification. Using the suggested technique, veins and arteries in retinal pictures were separated out based on the blood vessels tubular features. The author of [20] extracted the pixels of the vascular tree using a extractor based on morphology and topology operations and discovered topological vascular characteristics and relationships. A coarse-to-fine vascular identification approach for retinal pictures was put out in [21] by the author. This technique first applied generic vascular segmentation. Second, a more accurate segmentation of the vessels was carried out using morphological reconstruction and curvature analysis. These morphology-based techniques are quick, extremely effective, and effectively reduce noise. They do, however, heavily rely on the choice of structural components.

By integrating filter vessel tracking with firefly optimization operation, a vessel segmentation technique of fundus retinal pictures based on the optimized Frangi was suggested in this work. The fundus retinal picture underwent preliminary processing in order to isolate the green channel. Second, the use of CLAHE improved blood vessels. Third, blood vessel segmentation is performed. Last, classification is performed using KNN and SVM classifier.

.

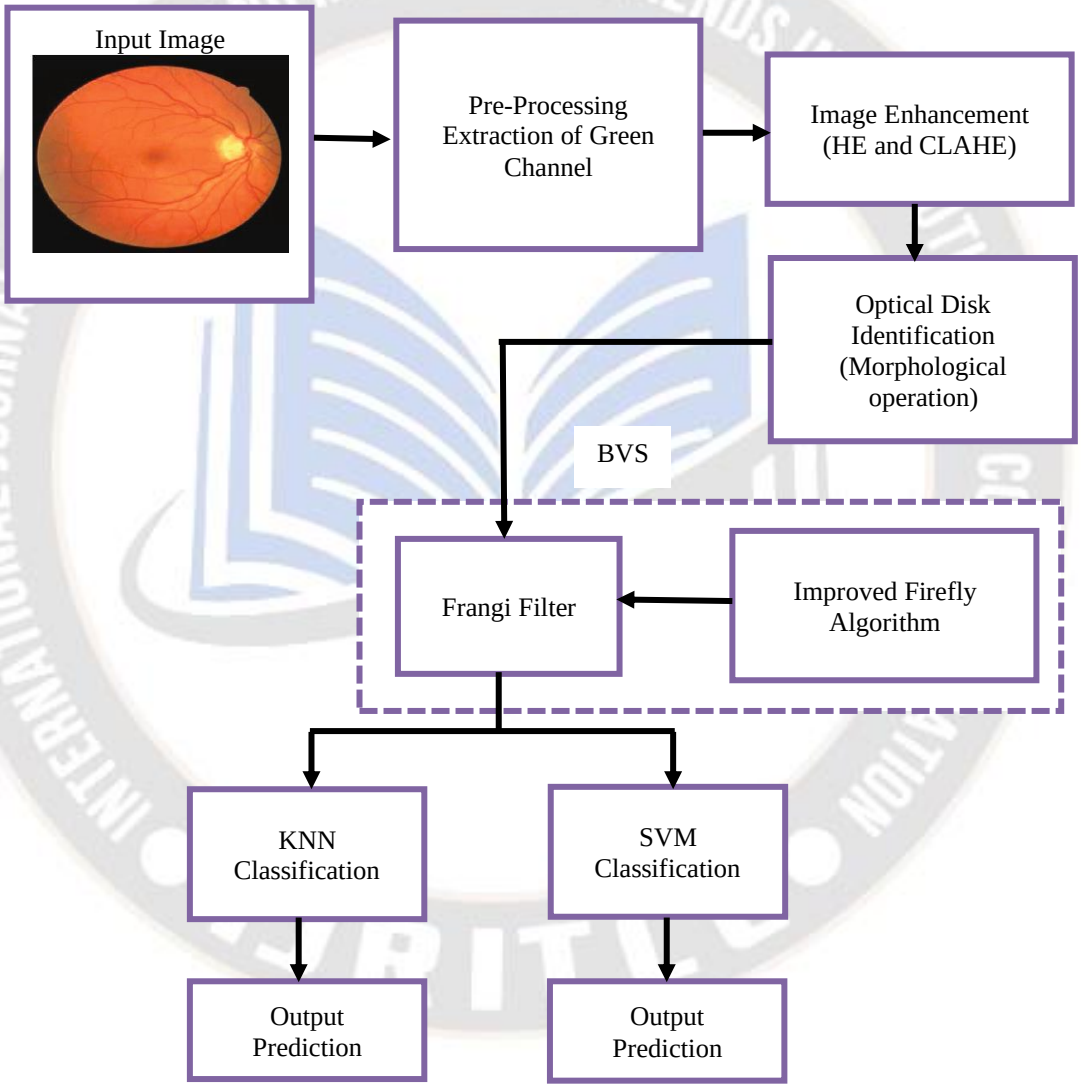

Figure 1. Proposed Model

II. Related Work

One of the four important primary treatments for blindness in the world is diabetic retina (DR). According to studies, up to 37.4% of people in China and India are blind due to severe retinopathy [22]. The eye's blood vessels are widely spaced throughout. Consequently, blood vessels are linked to eye abnormalities in most diabetes individuals. The segmentation of DR vascular pictures is important for the medical professionals' identification of the degree of diabetic retinopathy and subsequent therapy. The two primary types of current fundus vascular segmentation techniques are supervised

International Journal on Recent and Innovation Trends in Computing and Communication
ISSN: 2321-8169 Volume: 11 Issue: 9
***Article Received:** 25 July 2023 **Revised:** 12 September 2023 **Accepted:** 30 September 2023*

learning and unsupervised learning. Supervised learning typically requires an extensive training collection in which a model for training is periodically learned based on known images of the vascular pixel class in order to differentiate DR vascular photographs of unknown vascular pixel classes. Many academics have suggested a variety of neural network-based vessel segmentation techniques to enhance the approach of fundus vessel segmentation process. To accomplish autonomous extraction of vessel characteristics and boost algorithm accuracy, author suggested a deep learning methodology for segmenting fundus vessels [23].

The author in [24] designed a model for improving the segmentation accuracy in fundus images by combining the Gaussian filter and wave transform. The advancement of image processing technologies has coincided with the rise of artificial intelligence. The FCI assessment method employing the Spider Monkey Optimisation Algorithm (SMOA) was proposed by the author in [25]. Traditional threshold segmentation methods are based mostly on the OTSU algorithm, the greatest variance between classes criteria for separating pictures, and are unsupervised learning techniques.Among different approaches of segmentation OSTU model is easy to use when working with pictures that contain straightforward information.

The widespread arrangement of blood vessels in the fundus and the duplication of information precludes the single-threshold division method from achieving the project's objectives, thus it must be enlarged to a multi-threshold field. Computing intensive and tricky to use in practise, the OTSU approach for segmenting DR vascular images based on numerous criteria. Numerous academics have suggested employing population optimisation methods to resolve multi-threshold issues as a solution to this issue.

It is now simpler to execute multi-threshold segmentation of fundus vascular pictures in clinical practise thanks to a method the author of [26] presented utilising the Whale Optimisation Algorithm (WOA). Fundus photos with multiple thresholds are segmented by using Ant Colony Optimization (ACO), and the rate of accuracy in segmentation is increased by ACO's special pheromone update mechanism [27]. The matching filtered fundus picture of the DR is segmented by the author in [28] using Genetic process (GA) in an evolutionary process after additional blood vessel features have been preserved.

III. Materials and Method

Images are taken from the DRIVE [29], a database that is accessible to the general public, in order to assess the vessel detection methods. As it offers manual segmentations, the dataset named DRIVE is extensively utilized to evaluate the suggested methodology for segmentation of vessel. From the DRIVE database, ten retinal pictures are used, and criteria like sensitivity and specificity findings are compared with the industry benchmarks for each image. The proposed framework is shown in figure1. The example of drive dataset is shown in figure2.

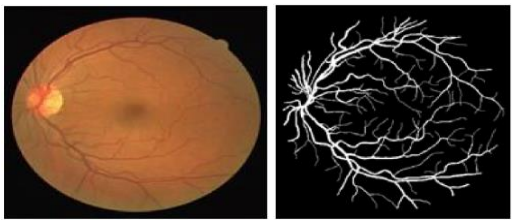

Figure 2. Drive Dataset with original image and ground truth image

A. Pre-Processing

The RGB format of fundus retinal pictures typically must be converted which makes the processing of data easy for diagnosis for which single channel images are developed. As shown in figure 3 the extracted images of R-Channel, G-Channel and B-Channel are displayed. The backdrop and blood arteries in the G channel picture contrast sharply. As a result, pre-processing was done on the G channel picture.

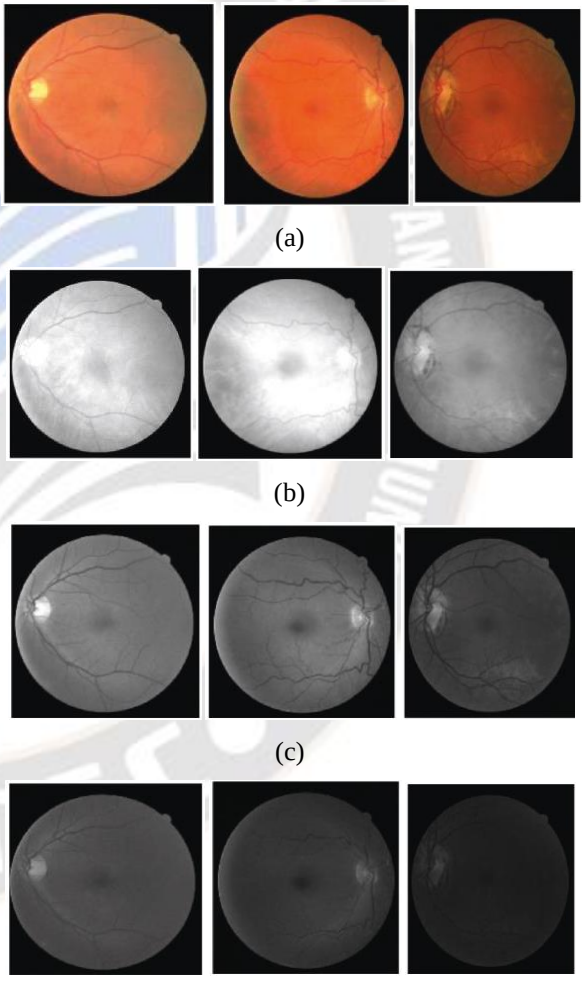

(a) Input image (b) R-Channel (c) G-Channel (d) B-channel
Figure 3. RGB extraction from colour image

B. Image Enhancement

A fundus retinal image's enhancement can help you recognise blood vessels apart from other background areas. A

International Journal on Recent and Innovation Trends in Computing and Communication
ISSN: 2321-8169 Volume: 11 Issue: 9
***Article Received:** 25 July 2023 **Revised:** 12 September 2023 **Accepted:** 30 September 2023*

specific image's histogram equalisation processing can improve the contrast of each item, broadening the range of the image's intensity. The global histogram equalisation approach falls short of achieving the desired augmentation of blood vessels as the vascular region is black and has little brightness in fundus retinal images.

By computing the transformation function of each pixel's neighbour domain, adaptive histogram equalisation (AHE) achieves histogram-enhancement of every pixel present in image. AHE is better suitable for improving picture edges and local contrast in order to obtain more information. AHE may enhance sounds surrounding small blood vessels in retinal vascular imaging while boosting contrast. Because the contrast-limited adaptive histogram equalisation (CLAHE) technique can prevent noise amplification, it is crucial to utilise it while enhancing retinal vasculature.Additionally, the CLAHE technique finds just one amplitude limit parameter using a straightforward computation. The processing of the CLAHE algorithm is shown in Figure. 4(b). The Figure.4 enhancement results were contrasted. While boosting the tiny blood vessels, the AHE algorithm amplified the sounds in the picture backdrop and around them. The image's uneven brightness distribution was caused by this characteristic. The CLAHE algorithm, on the other hand, substantially reduced the interferences of noise and improving the contrast among the blood vessels and backdrop.

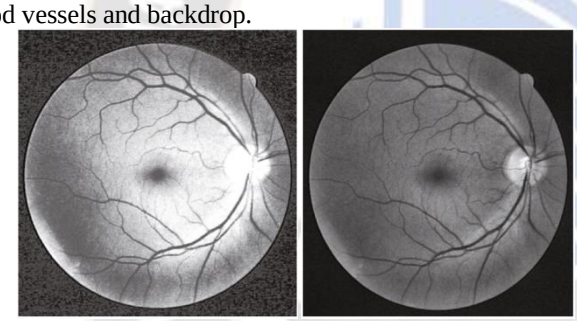

(a) (b)

Figure 4. Image Enhancement (a) using histogram equalization (b) using CLAHE

C. Optic Disk Identification and Separation

The advantages of having a system that can automatically identify this disease's early warning symptoms have been thoroughly investigated and favourably evaluated. As a result, the OD is crucial in the development of automated diagnostic expert systems for DR since many algorithms used to identify other fundus traits rely heavily on the segmentation of the OD. To find the OD, morphological operation is used. The background area of the picture has its noise interference removed once the OD has been located.

The structural components of the eye are applied to each binary picture pixel during dilatation. Every time a structural element's origin and are combined with binary pixels so that the overall structural element is wrapped up, and the accompanying binary image pixels are then changed. The output which was initially initialised to zero is a binary image and is written with the results of the logical addition. When applying structural erosion, the element additionally traverses each picture pixel. If, at some point, every single pixel structuring element correlates with a single pixel binary image, then the centre pixel structuring element logically disjuncts from the corresponding pixel in the output picture.

The mathematical approach of morphological operation is given as,

$$D_I = I_o \otimes E_s \quad (1)$$

$$E_I = I_o \ominus E_s \quad (2)$$

whereI_o is original image which is given as input, E_s is a structural element, and image after dilation is termed as $D_I$and image after erosion is termed asE_I.

In the process of morphology operation, the term "open" describes the erosion of the picture using the E_s and the subsequent application of the dilation operation. Without compromising other features, bright regions of the image that are smaller than structural elements can be removed using an open technique.

$$O_I = I_o \circ E_s \quad (3)$$

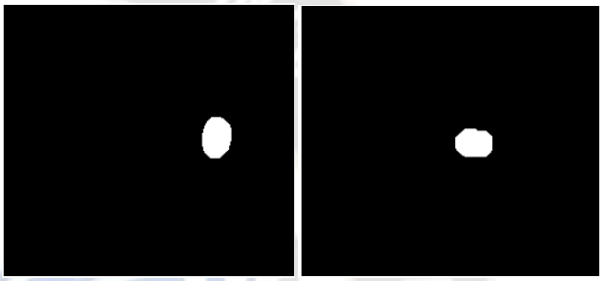

Figure 5. Region of optical Disk

Due to the green channel's suitability for blood vessel detection in the retinal picture, vessels with an OD border are recognised and segregated from the green channel shown in figure 5.

D. Blood vessel Segmentation

After identification of optical disk, blood vessel segmentation (BVS) is performed. For this BVS proposed an optimized frangi filter. The filter is optimized using improved firefly algorithm. Figure 6 shows the blood vessel segmented image.

The effectiveness of vessel segmentation may be significantly impacted by the attainment of enhancing filters. The most common methods for vessel improvement depend on the second order derivate of the image and the differential information of the image. The research is often carried out over a variety of scales since the vessels occur in varied sizes.

If Io(x,y) stands for the original picture, then the scaled-down Hessian of Io(x,y)is

$$H_e(x,y,s) = s^2 I_o(x,y) * \frac{\partial^2}{\partial x \partial y} G(x,y,s))$$

$$Gf(x,y,s) = (2\pi s^2)^{-1/2} \exp\left(-\frac{x^2+y^2}{2s^2}\right) \ldots . (4)$$

Represented by [30],

Here Gf(x,y,s) is termed as the gaussian function having a ‘k’ kernel size. To take into consideration varied picture spacing for various dimensions, the kernel size may be changed. It makes natural sense to examine the sizes and signs of the Hessian eigenvalues (HEV) in the framework of vessel detection. The local picture structures can be made better by analysing the magnitudes and signs of the HEV.

International Journal on Recent and Innovation Trends in Computing and Communication
ISSN: 2321-8169 Volume: 11 Issue: 9
***Article Received:** 25 July 2023 **Revised:** 12 September 2023 **Accepted:** 30 September 2023*

The Hessian matrix (HM) eigenvalues are derived by eigenvalue decomposition, i.e.,eig He(x,y,s) → λ _i,i=1,2Depending on the magnitude values the eigen values are sorted out i.e., | λ _1 |≤| λ _2 |The following connection indicates the vessel-like shapes in the picture that we are fascinated in,λ_1the smaller value (which is ideally zero), and |λ_1 |<<|λ_2 |.

Additionally, negatives values are seen when the vessels are glowing tubular structures in a three-dimensional space. The potential of extra components in the image is ruled out using this sign data as a reliability analysis. The eigenvalues of the HM serve as the foundation for several vesselness functions. Frangi et al. [12] used the ratio of eigenvalues to define the vesselness function V_frangi.

$$V_{Frangi} = \begin{cases} 0 & if\ \lambda_2 > 0, \\ \exp\left(-\frac{\left(\frac{\lambda_1}{\lambda_2}\right)^2}{2\delta^2}\right)\left(1-\exp\left(-\frac{\lambda_1^2+\lambda_2^2}{2\omega^2}\right)\right) & otherwise \end{cases} \ldots(5)$$

The unambiguous concentration of the functions on λ1and λ2 reduces response uniformity and makes them extremely sensitive to picture contrast. Additionally, the function's response is subpar for smaller values of λ2. It is hence extremely susceptible to picture noise. Author in [30] proposed an enhanced vesselness function V as follows to address this,

Where λp is computed as below,

In this case, the value of λ2 is regularised at every level s to guarantee the vesselness function's resilience against lower-level magnitudes of λ_2.τranges from [0 1] which is a cut-off

$$V = \begin{cases} 0 & if\ \lambda_2 > 0 \\ \lambda_2^2(\lambda_\rho - \lambda_2)\left(\frac{3}{\lambda_2+\lambda_\rho}\right)^3 & if\ \lambda_2 \le {}^{\lambda_\rho}/_2 \\ 1 & otherwise \end{cases} \quad (6)$$

$$\lambda_\rho = \begin{cases} \lambda_2 & if\ \lambda_2 < \tau min_{x,y}\lambda_2(x,y,s) \\ \tau min_{x,y}\lambda_2(x,y,s) & otherwise \end{cases} \quad (7)$$

threshold. For negative eigen values, it is necessary to highlight the brilliant structures on the dark backdrop.Therefore$\lambda_2$with higher magnitude is obtained as $\min_{x,y}\lambda_2(x,y,s)$. At several scales, the vesselness function in Eq. (7) is investigated. The filter's reaction will peak at a scale that closely resembles the size of the target vessel. To create an improved picture estimate, we integrate the measure of vesselness offered by the response of filter at various

$$I_{enhanced}(x,y) = \max_{s_{min} \le s \le s_{max}}(V) \quad (8)$$

scales$I_{enhanced}(x,y)$ as:

Where s_{min} and s_{max}establish the scale range and are chosen based on the minimum and maximum anticipated sizes of the structures of concern.

Improved Firefly optimized

Because they are unisex, the attraction of fireflies is irrespective of their sexes. The attraction of fireflies is inversely correlated with light intensity, and it diminishes with the increase in distance. For any pair of flashing fireflies, the less brilliant one will go towards the more dazzling one. It will move arbitrarily if there is not another firefly that is more brilliant than the one in question.

Algorithm

The implementation procedure of the proposed firefly algorithm (FA) can be stated below:

S1: Generate the firefly's population$\{x_1, x_2, \ldots\ldots, x_n\}$.
S2: Evaluate brightness value for every firefly
S3: Updating of each firefly.
S4: Fireflies intensity are given as $\{I_1, I_2, \ldots\ldots, I_n\}$
S5: Ranking the fireflies and find best of the present
S6: Moving every firefly I towards other brighter fireflies.
S7: Stop when criterion is fulfilled; otherwise go to S2

Parameters used in Firefly Algorithm

- *Measure of Distance:*

Measure of distance is observed between two fireflies (i, j) and their positions (x_i, x_j) and the distance is termed as Cartesian or Euclidean distance $r_{ij}$and is given by,

$$r_{ij} = \|x_i - x_j\| = \sqrt{\sum_{k=1}^{d}(x_{i,k} - x_{j,k})^2} \quad (9)$$

Where$x_{i,k}$ is the intensity of a firefly and k is the k^{th} component of the spatial coordinate$x_i$of thei^{th} firefly.

Attractiveness:

The variation of attractiveness β with distance r by

$$\beta = \beta_o \quad (10)$$

where β_o is the attractiveness at r =0.

γ is attractive coefficient.
r is the distance between two fireflies.

- *Movement*

A firefly i that is drawn to another more attractive (brighter) firefly j moves as a result of and is given by

$$X_i^{t+1} = x_i^t + \beta_o e^{-\gamma r_{ij}^2}\left(x_j^t - x_i^t\right) + \alpha_t \varepsilon_i^t \quad (11)$$

In equation 11 the entire second term is based on the attraction parameter. Random term is said to be the third term with α being the parameter of randomization and ε_i^t it is a vector of random numbers.

The Hessian matrix's eigenvalues λ_2 and λ_ρ are necessary for computing the vesselness function.These eigen values are optimized using firefly optimization to improve the performance of frangi filter.

$$\varphi_{opt} = \underset{s_{min}, s_{max}, k, \tau}{\arg\max}\left\{EV\left(I_{enhance}(x,y)\right)\right\} \quad (12)$$

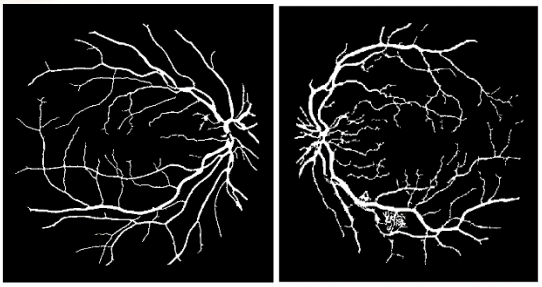

Figure 6. Blood vessel segmented images

International Journal on Recent and Innovation Trends in Computing and Communication
ISSN: 2321-8169 Volume: 11 Issue: 9
Article Received: *25 July 2023* ***Revised:*** *12 September 2023* ***Accepted:*** *30 September 2023*

E. Feature Extraction

The extraction of a grayscale picture serves as the foundation for the Gray-Level Co-occurrence Matrix (GLCM). The GLCM algorithms calculate the frequency of pairings of pixels with specific amounts and in a specific spatial arrangement appearing in an image, generating a GLCM, and then extract statistical characteristics that describe the texturing of a picture from this matrix.

GLCM is a well-liked texture-based feature extraction method. This method performs an operation on the images based on second-order statistics to ascertain the texture of the connection between pixels. Ordinarily, two pixels are used for this procedure. The frequency of these pixels' intensity combinations is determined by the GLCM algorithm. In other words, this method represents the frequency at which pixel pairings occur. The representation of GLCM traits of an image is in matrix format with i-rows and j-columns as the grey values of an image.

The frequency of the two pixels is used by the matrix's components. The neighborhood may affect both pixel pairs differently. The second-order statistical probability values that depend on the grayscale of the rows and columns are included in these matrix members. Wide intensity levels cause the transient matrix to grow significantly. A time-consuming process load results from this.

Contrast: It is a metric that evaluates the intensity of the whole image by considering the contrast of pixel and its neighbour pixels. The contrast value is zero for a constant image.

$$Contrast = \sum_{i,j} |i-j|^2 p(i,j) \qquad (13)$$

Correlation: The correlation relation of pixel with its neighbour pixel of an image. The range of correlation value is -1 to1. For constant image the correlation is not taken into consideration. If the value is 1 the image is positively correlated and if value is -1 the image is negatively correlated image.

$$Correlation = \sum_{i,j} \frac{(i-\mu i)(j-\mu j)p(i,j)}{\sigma_i \sigma_j} \qquad (14)$$

Energy: The sum of squared elements of the pixels in an image with i-rows and j-columns gives the energy trait of GLCM. The value of energy is 1 for constant image.

$$Energy = \sum_{i,j} p(i,j)^2 \qquad (15)$$

F. Classification

$$Homogeneity = \sum_{i,j} \frac{p(i,j)}{1+|i-j|} \qquad (16)$$

To determine the stage of diabetic retinopathy (DR), characteristics of the vessels were acquired. Here, we discovered the retinal vessels' pixel density. The KNN and SVM classifiers receive these characteristics as input. To identify the existence of DR, the class produced by the KNN and SVM classifier is employed. Figures 7 and 8 represents the KNN and SVM classification process.

KNN

For the categorization of diabetes and non-diabetic pictures, the KNN classifier is used. KNN (K-Nearest Neighbours) is a prominent ML (Machine Learning) method that is widely utilised. This algorithm successfully accomplishes classification. Unsupervised machine learning is the term used to describe this approach. The K-NN technique to classification and regression is non-parametric. One of the techniques used in the guided learning process is K-NN. The basic concept behind this method is to identify data by calculating a data point's k closest neighbours. To put it another way, figure out where the test results and the feedback differ and then make the proper forecast. Most K-NN classifiers assess the distance between samples given as vector inputs using simple Euclidean metrics.

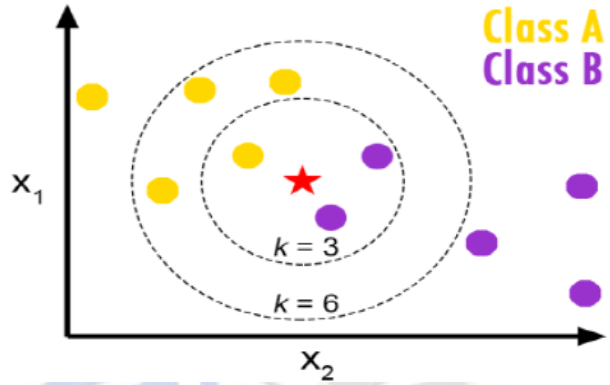

Figure 7. KNN Classification process

SVM

The Support Vector Machine (SVM) technique was created for pattern classification but has lately been modified for additional applications including estimating distributions and discovering regression. The challenge is to find a hyper-plane that separates the data points by as little space as possible. Positive or negative data points are assigned to the data points. In a high- or infinite-dimensional domain, SVM creates a hyper plane or group of hyper planes that may be utilised for classification.

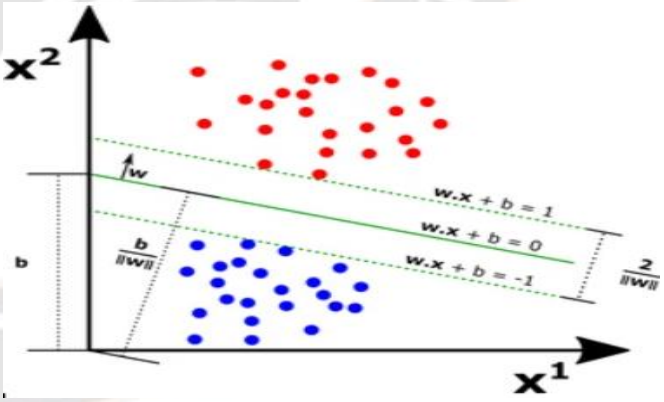

Figure 8. SVM Classification process

The explanation of SVM with an exemplary. Considering a set i.e.,$\{(a_1, b_1), (a_2, b_2), \ldots, (a_r, b_r)\}$,is an vector input in $A \subseteq R^n$and the value of output is b_i, $b_i \in \{1,0\}$. The positive class is termed as '1'and the negative class is termed as '0'. From this the linear function of SVM is in the form of $f(a) = (w.a) + k$

$$b_i = \begin{cases} 1 \; if \; (w.a_i) + k \geq 0 \\ 0 \; if \; (w.a_i) + k < 0 \end{cases} \qquad (17)$$

International Journal on Recent and Innovation Trends in Computing and Communication
ISSN: 2321-8169 Volume: 11 Issue: 9
***Article Received:** 25 July 2023 **Revised:** 12 September 2023 **Accepted:** 30 September 2023*

IV. Experimental Evaluation

This study offers a brand-new method for identifying diabetic retinopathy. Regarding several aspects, such as accuracy, precision, and sensitivity, the new approach is compared to the older algorithm. DRIVE database, a publicly available retinal image database, is used to assess the proposed study. 40 colour retinal pictures in two sets—training and testing—make up the DRIVE (Digital Retinal pictures for Vessel Extraction) database. A training set is not required because the offered approach is unsupervised. Twenty photos, masks, and manually identified vessel structures or ground truth are included in the testing set. The results obtained for image1 is shown in figure9.

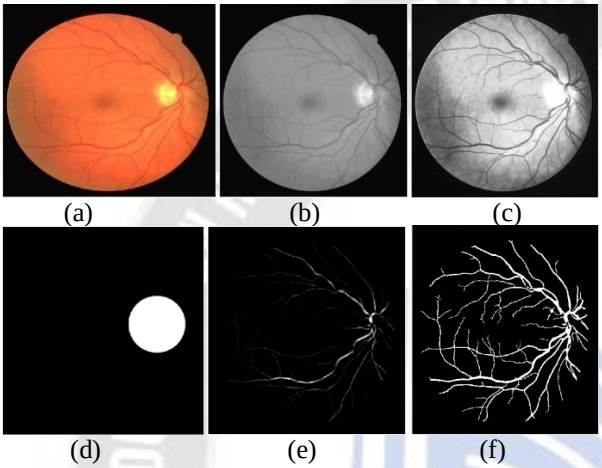

Figure 9. Results of RBVS for image1 (a) original image (b) Extracted G channel (c) CLAHE Enhanced (d) Optical disk extraction (e) Frangi filter BVS (f) FOFF BVS

The parameters evaluated are accuracy, sensitivity, and precision. All these parameters are evaluated using the values based on truly positive (TP), truly negative (TN), falsely positive (FP) and falsely negative (FN). The term TP determines the correct match in count of vessel pixels. TN determines the correct match in count of background pixels. The FP determines the count of backdrop pixels. FN determines the count of vessel pixels. The evaluated metrics are provided to gauge the accuracy value of the output segmented based on these counts. One of the most used metrics to gauge how effective the segmented result is accuracy (Acc). It demonstrates how well the system is at recognizing the pixels background and the vessel. Its definition is the percentage of correctly detected background and vessel pixels to all the pixels. Mathematically, it is formulated as,

$$\text{Acc} = \frac{\text{TP+TN}}{\text{TP+TN+FP+FN}} \quad (18)$$

$$\text{Sen} = \frac{\text{TP}}{\text{TP+FN}} \quad (19)$$

$$\text{Precision} = \frac{\text{TN}}{\text{FP+TN}} \quad (20)$$

TABLE1. PARAMETERS EVALUATED FOR DIFFERENT IMAGES USING FOFF-KNN

Images	Accuracy	Sensitivity	Precision
I1	91.6	96.8	92.9
I2	90.8	96.2	92.2
I3	91.2	95.9	92.3
I4	91.4	96.0	91.9
I5	90.9	96.1	92.1
Avg	91.2	96.2	92.3

TABLE2. PARAMETERS EVALUATED FOR DIFFERENT IMAGES USING FOFF-SVM

Images	Accuracy	Sensitivity	Precision
I1	95.5	99.8	94.7
I2	94.8	99.1	94.3
I3	95.1	98.9	93.9
I4	95.3	99.7	94.0
I5	95.0	99.6	94.5
Avg	95.2	99.4	94.3

When compared to existing techniques, the proposed methodology in this paper shows promising results and are tabulated in table3.

TABLE3. COMPARISON OF PARAMETERS USING DIFFERENT TECHNIQUES

Author& Year		Dataset	Accuracy	Sensitivity	Precision
Panda et al., (2016) [31]		DRIVE	95.0	99.2	68.2
Zhang et al., (2016) [32]		DRIVE	95.1	97.1	79.7
Pandey et al., (2017) [33]		DRIVE	95.5	96.2	80.3
Ramos et al., (2018) [34]		DRIVE	92.6	96.05	72.24
Rocha et al., (2020) [35]		DRIVE	94.8	95.7	83.3
Proposed	***FOFF-KNN***	**DRIVE**	**91.66**	**96.84**	**92.9**
	FOFF-SVM	**DRIVE**	**95.50**	**99.7**	**94.7**

To distinguish each pixel as a vessel pixel is the primary goal of segmenting retinal blood vessels. The output of segmented image using the proposed method is contrasted with the associated original ground truth image. Using a confusion matrix, the technique's effectiveness is evaluated. The confusion matrix displays the ratio of accurate guesses to inaccurate predictions. Figure 10 & Figure 11 shows the confusion matrix of SVM and KNN classifiers.

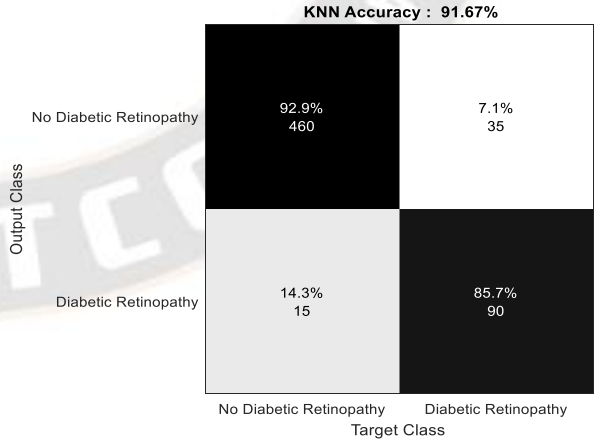

Figure 10. Confusion Matrix using KNN classifier

International Journal on Recent and Innovation Trends in Computing and Communication
ISSN: 2321-8169 Volume: 11 Issue: 9
***Article Received:** 25 July 2023 **Revised:** 12 September 2023 **Accepted:** 30 September 2023*

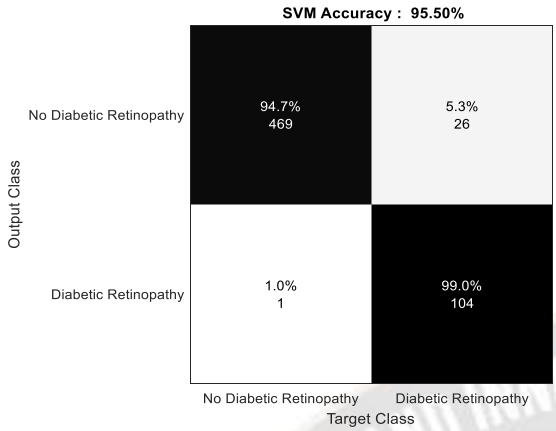

Figure 11. Confusion Matrix using SVM classifier

IV. CONCLUSION

An ophthalmologist can identify diabetic retinopathy using automated assessment of the condition that is based on computerized BVS in retinal images. The acquired photos from the DRIVE database were used to extract the blood vessels of retina for this study. For more research on diabetic retinopathy, vessel extraction is crucial. Additionally, the development of vessels helps identify the degree and stage of diabetic retinopathy. Based on FOFF-KNN and FOFF-SVM, a novel classification method for retinal blood vessels is used. On the impacted photos, the suggested model is evaluated to demonstrate its superiority to the ones now in use. An accuracy of 95.5%, sensitivity 99.7% and precision 94.7% are found in enhanced based images with FOFF methods.

REFERENCES

[1] M. Niemeijer, J. Staal, B. van Ginneken, M. Loog, and M. D.Abramoff, "Comparative study of retinal vessel segmentationmethods on a new publicly available database. Medical Imaging2004: Image Processing," International Society for Opticsand Photonics, vol. 5370, pp. 648–656, 2004.

[2] R. Khanduzi and A. K. Sangaiah, "A fast genetic algorithm fora critical protection problem in biomedical supply chain networks,"Applied Soft Computing, vol. 75, pp. 162–179, 2019.

[3] F. Al-Turjman, M. H. Nawaz, and U. D. Ulusar, "Intelligencein the Internet of Medical Things era: a systematic review ofcurrent and future trends," Computer Communications, vol. 150, pp. 644–660, 2019.

[4] S. Chaudhuri, S. Chatterjee, N. Katz, M. Nelson, andM. Goldbaum, "Detection of blood vessels in retinal imagesusing two-dimensional matched filters," IEEE Transactionson Medical Imaging, vol. 8, no. 3, pp. 263–269, 1989.

[5] Q. Li, J. You, and D. Zhang, "Vessel segmentation and widthestimation in retinal images using multiscale production ofmatched filter responses," Expert Systems with Applications,vol. 39, no. 9, pp. 7600–7610, 2012.

[6] J. Kaur and H. P. Sinha, "Automated detection of retinal bloodvessels in diabetic retinopathy using Gabor filter," InternationalJournal of Computer Science and Network Security(IJCSNS), vol. 12, no. 4, p. 109, 2012.

[7] X. H. Wang, Y. Q. Zhao, M. Liao et al., "Automatic retinal vesselsegmentation based on multiscale 2D Gabor wavelet," Journalof Automation, vol. 41, no. 5, pp. 970–980, 2015.

[8] N. P. Singh and R. Srivastava, "Extraction of retinal blood vesselsby using an extended matched filter based on secondderivative of Gaussian," Proceedings of the National Academy of Sciences, India Section A: Physical Sciences, vol. 89, no. 2,pp. 269–277, 2019.

[9] I. Cruz-Aceves, F. Oloumi, R. M. Rangayyan, J. G. Aviña-Cervantes,and A. Hernandez-Aguirre, "Automatic segmentationof coronary arteries using Gabor filters and thresholding basedon multi-objective optimization," Biomedical Signal Processingand Control, vol. 25, pp. 76–85, 2016.

[10] H. Aguirre-Ramos, J. G. Avina-Cervantes, I. Cruz-Aceves,J. Ruiz-Pinales, and S. Ledesma, "Blood vessel segmentationin retinal fundus images using Gabor filters, fractional derivatives,and expectation maximization," Applied Mathematicsand Computation, vol. 339, pp. 568–587, 2018.

[11] N. P. Singh and R. Srivastava, "Retinal blood vessels segmentationby using Gumbel probability distribution function basedmatched filter," Computer Methods and Programs in Biomedicine,vol. 129, pp. 40–50, 2016.

[12] A. F. Frangi, W. J. Niessen, K. L. Vincken, and M. A. Viergever,Multiscale Vessel Enhancement Filtering. International Conferenceon Medical Image Computing and Computer-AssistedIntervention, Springer, Berlin, Heidelberg, 1998.

[13] D. Kumar, A. Pramanik, S. S. Kar, and S. P. Maity, "Retinalblood vessel segmentation using matched filter and Laplacianof Gaussian," in International Conference on Signal Processingand Communications (SPCOM), pp. 1–5, Bangalore, India,2016.

[14] A. Fathi and A. R. Naghsh-Nilchi, "Automatic wavelet-basedretinal blood vessels segmentation and vessel diameter estimation,"Biomedical Signal Processing and Control, vol. 8, no. 1,pp. 71–80, 2013.

[15] Y. Qian Zhao, X. Hong Wang, X. Fang Wang, and F. Y. Shih,"Retinal vessels segmentation based on level set and regiongrowing," Pattern Recognition, vol. 47, no. 7, pp. 2437–2446,2014.

[16] K. Rezaee, J. Haddadnia, and A. Tashk, "Optimized clinicalsegmentation of retinal blood vessels by using combinationof adaptive filtering, fuzzy entropy and skeletonization,"Applied Soft Computing, vol. 52, pp. 937–951, 2017.

[17] R. Ghoshal, A. Saha, and S. Das, "An improved vessel extractionscheme from retinal fundus images," Multimedia Toolsand Applications, vol. 78, no. 18, pp. 25221–25239, 2019.

[18] Y. Zhao, L. Rada, K. Chen, S. P. Harding, and Y. Zheng, "Automatedvessel segmentation using infinite perimeter active contourmodel with hybrid region information with application toretinal images," IEEE Transactions on Medical Imaging,vol. 34, no. 9, pp. 1797–1807, 2015.

[19] L. C. Rodrigues and M. Marengoni, "Segmentation of opticdisc and blood vessels in retinal images using wavelets, mathematicalmorphology and Hessian-based multi-scale filtering,"Biomedical Signal Processing and Control, vol. 36, pp. 39–49,2017.

[20] J. Rodrigues and N. Bezerra, "Retinal vessel segmentationusing parallel grayscale skeletonization algorithm and mathematicalmorphology," in 29th SIBGRAPI Conference onGraphics, Patterns and Images (SIBGRAPI), pp. 17–24, SaoPaulo, Brazil, 2016.

[21] L. Câmara Neto, G. L. B. Ramalho, J. F. S. Rocha Neto, R. M. S.Veras, and F. N. S. Medeiros, "An unsupervised coarse-to-finealgorithm for blood vessel segmentation in fundus images,"Expert Systems with Applications, vol. 78, pp. 182–192, 2017.

[22] P. Prasanna, P. Samiksha, K. Ravi et al., "Indian diabeticretinopathy image dataset (IDRiD): a database for diabeticretinopathy," Screening Research Data, vol. 3, no. 3, 2018.

[23] L. Xie, Study on Vascular Segmentation Method of FundusImage Based on Deep Learning, Shenzhen University,Shenzhen, China, 2017.

[24] X. Fan, Vessel Segmentation Based on Wavelet Transform andSteerable Gaussian Filter in Fundus Image, Suzhou University,Suzhou, China, 2018.
[25] V. Rajinikanth, H. Lin, J. Panneerselvam, and N. Sri MadhavaRaja, "Examination of retinal anatomical structures—a studywith spider Monkey optimization algorithm," in Applied Nature-Inspired Computing: Algorithms and Case Studies,N. Dey, A. S. Ashour, and S. Bhattacharyya, Eds., SpringerSingapore, Singapore, 2020.
[26] J. Nasiri and F. M Khiyabani, "A whale optimization algorithm(WOA) approach for clustering," Cogent Mathematics& Statistics, vol. 5, no. 1, Article ID 1483565, 2018.
[27] R. Arnay, F. Fumero, and S. Jose, "Ant Colony Optimizationbasedmethod for optic cup segmentation in retinal images,"Applied Soft Computing, vol. 52, 2017.
[28] M. Al-Rawi and H. Karajeh, "Genetic algorithm matched filteroptimization for automated detection of blood vessels fromdigital retinal images," Computer Methods and Programs in
[29] Biomedicine, vol. 87, no. 3, pp. 248–253, 2007.J. Staal and M. D. Abramoff, "Ridge-based vessel segmentation in colorimages of the retina," IEEE Trans. Med. Imaging 23(4), 501–509 (2004).
[30] Jerman T, Pernuš F, Likar B, Špiclin Ž. Beyond Frangi: an improved multiscalevesselness filter. In Medical Imaging 2015: Image Processing 2015 Mar 20; 9413: 623-633.
[31] Panda R, Puhan NB, Panda G. New binary Hausdorff symmetry measure based seeded region growing for retinal vessel segmentation. Biocybernetics and Biomedical Engineering. 2016 Jan 1; 36(1):119-29.
[32] Zhang J, Dashtbozorg B, Bekkers E, Pluim JP, Duits R, terHaarRomeny BM. Robust retinal vessel segmentation via locally adaptive derivative frames in orientation scores. IEEE Transactions on Medical Imaging. 2016 Aug 3; 35(12):2631-44.
[33] Pandey D, Yin X, Wang H, Zhang Y. Accurate vessel segmentation using maximumentropy incorporating line detection and phase-preserving denoising. Computer Vision andImage Understanding. 2017 Feb 1; 155:162-72.
[34] Aguirre-Ramos H, Avina-Cervantes JG, Cruz-Aceves I, Ruiz-Pinales J, Ledesma S. Blood vessel segmentation in retinal fundus images using Gabor filters, fractional derivatives, and Expectation Maximization. Applied Mathematics and Computation. 2018 Dec 15; 339:568-87.
[35] Rocha DA, Barbosa AB, Guimarães DS, Gregório LM, Gomes LH, da Silva Amorim L, Peixoto ZM. An unsupervised approach to improve contrast and segmentation of blood vessels in retinal images using CLAHE, 2D Gabor wavelet, and morphological operations. Research on Biomedical Engineering. 2020 Mar; 36(1):67-75.